Geomechanics and Engineering, *Vol. 39, No. 2 (2024) 181-195*
https://doi.org/10.12989/gae.2024.39.2.181

Effects of pile tip cutting due to shield TBM tunnel construction on pile behaviour under various reinforcement conditions

Young-Jin Jeon[1a], Seung-Kueon Seo[2b], Young-Nam Choi[3c], Ho-Yeol Son[4d], Byung-Soo Park[5e], Jae-Hyun Kim[6f] and Cheol-Ju Lee*[6]

[1]*College Institute of Industrial Technology, Kangwon National University, 1 Kangwondaehak-gil, Chuncheon-si, Gangwon-do, Republic of Korea*
[2]*Hence Company Limited, 63 gil 45, Poongseong-ro, Gangdog-gu, Seoul, Republic of Korea*
[3]*Center for Climate Change Research, Chungnam Institute, 360, Hongye-ro, Hongbuk-eup, Hongseong-gun, Chungcheongnam-do, Republic of Korea*
[4]*Pyeonghwa Dam Office, K-water, 3481-18, Pyeongwa-ro, Hwacheon-eup, Hwacheon-gun, Gangwon-do, Republic of Korea*
[5]*Department of Civil Engineering, Gangwon State University, 270 Yeonju-ro, Jumunjin-eup, Gangneung-si, Gangwon-do, Republic of Korea*
[6]*Department of Civil Engineering, Kangwon National University, 1 Kangwondaehak-gil, Chuncheon-si, Gangwon-do, Republic of Korea*

(*Received August 25, 2024, Revised October 5, 2024, Accepted October 7, 2024*)

Abstract. Existing piles, especially in urban areas, are at risk of being cut by new tunnel construction, potentially affecting their serviceability. This study examined the behaviour of piles under various reinforcement conditions subject to tip cutting resulting from tunnel excavation. For this, the construction of a tunnel using a shield tunnel boring machine adjacent to existing single and group piles was simulated. A three-dimensional finite element analysis was used to perform the simulations. Certain piles in the group were simulated by cutting the pile tips to mimic the effect of tunnel excavation, and the behaviour of the piles was studied by considering the effect of pile cap and ground reinforcements. A numerical analysis was used to examine the ground settlement caused by tunnel excavation, pile head settlement, axial pile force, and shear stress occurring at the pile–ground interface. The results revealed that for all piles with pile tips supported by weathered rock, the shear stress distributions demonstrated similar trends, whereas for piles with cut tips, tensile or compressive forces occurred simultaneously according to the relative position by pile depth. Additionally, when the pile tip was supported by weathered rock, approximately 70% of the support was due to shaft friction and the remaining 30% was provided by the pile tip. For piles without reinforcement, the final settlement was approximately 70% greater than that of piles with grouting reinforcement. These results indicate that pile and ground settlements are substantially influenced by pile tip cutting and reinforcement conditions.

Keywords: numerical analysis; pile cutting; pile behaviour; reinforcement conditions; shield TBM

1. Introduction

In recent years, the various tunnel construction projects undertaken to build convenient infrastructure in densely populated urban areas have induced ground settlement. Previous research has indicated that settlement of the ground surrounding tunnel excavation is inevitable, causing the deformation of pile structures adjacent to the tunnel and altering the axial force distribution, thus significantly impacting the behaviour of the piles and their serviceability (Lee 2012a). To address the problems associated with pile behaviour changes caused by tunnel excavation, researchers have conducted numerous studies, including numerical analyses, theoretical research, indoor model tests, and centrifugal model tests (Jacobsz 2002, Pang 2006, Cheng *et al*. 2007, Lee and Chiang 2007, Marshall 2009, Lee 2012a, b, c, Lee 2013, Ng *et al*. 2013, Dias and Bezuijen 2014a, b, Hartono *et al*. 2014, Liu *et al*. 2014, Ng and Lu 2014, Ng *et al*. 2014, Williamson 2014, Hong *et al*. 2015, Jeon and Lee 2015, Jeon *et al*. 2015, Lee *et al*. 2016, Jeon *et al*. 2017, Jeon *et al*. 2018, Soomro *et al*. 2018, Jeon *et al*. 2020a, b, Zhang *et al*. 2021, Jeon *et al*. 2022, Wang and Yuan 2022, Jeon and Lee 2023). In contrast, field measurement studies are relatively limited. However, Selemetas (2005), Pang (2006), Liu *et al*. (2014), Mair and Williamson (2014), Williamson (2014), and Selemetas and Standing (2017) conducted field measurements to study the effects of tunnel excavation on the behaviour of adjacent piles. Fig. 1 illustrates a typical cross-section of the Bangkok Metropolitan Rapid Transit (MRT) tunnel constructed by an earth pressure balance machine that passes between bridge piles in Bangkok, as presented by Phienwej *et al*. (2006). Approximately 339 pile structures were monitored during the tunnel excavation. They found that for piles located above the tunnel, the pile head settlement ranged from

*Corresponding author, Professor
E-mail: cj32@kangwon.ac.kr
[a]Senior Researcher
[b]President
[c]Senior Researcher
[d]Manager
[e]Professor
[f]Professor

ISSN: 2005-307X (Print), 2092-6219 (Online)

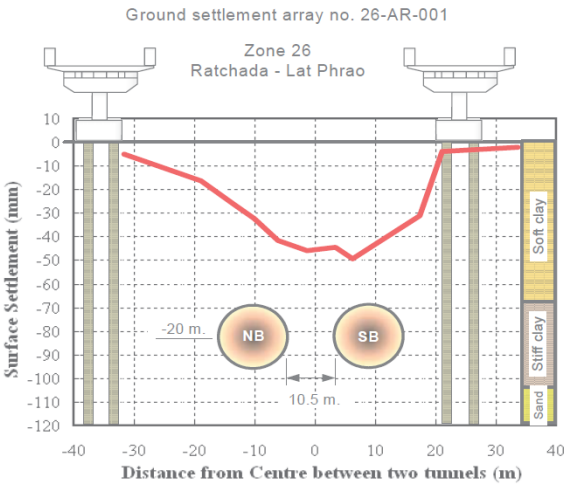

Fig. 1 Cross-section of the Bangkok MRT between bridge piles (Phienwej *et al*. 2006)

approximately 20 to 40 mm. However, when the tunnel passed alongside the piles, the pile head settlement was less than 10 mm. Consequently, appropriate measures should be established because pile settlement is highly dependent on the relative position of a tunnel to the surrounding piles.

Recently, the shield tunnel boring machine (TBM) method has emerged as the optimal method for minimising ground deformation and civil complaints. The shield TBM method applies face pressure during excavation to minimise ground settlement and has the advantage of shortening construction time through a continuous process of segment assembly and grouting during excavation. Kaalberg *et al*. (2005) conducted field measurements and a numerical analysis using the TBM method to determine the impact of tunnel excavation on ground and pile settlements. They compared the influence zones of ground settlement due to tunnel excavation by considering the relative position of the tunnel to the pile tip. Williamson (2014) studied the influence zones of ground settlement due to tunnel excavation and reported that piles within the influence zone had a lower apparent factor of safety than those outside the influence zone. The explanation for this phenomenon was unclear, thus necessitating a systematic study. Thus, Mroueh and Shahrour (2008) simulated TBM excavation with constant face pressure through numerical analysis, examining surface settlement and changes in the ground near the tunnel. Moreover, Jeon *et al*. (2018) simulated the shield TBM method under varying face pressures using a numerical analysis to study the pile behaviour during close-proximity tunnel construction. Furthermore, the researchers at Cambridge University monitored the behaviour of under-reamed piles partially cut during tunnel excavation. They used vibration sensors to detect changes in the axial pile forces and evaluated pile stability through data collection and analysis. Finally, they concluded that monitoring the behaviour of piles subject to tunnel excavation played a significant role in maintaining pile stability (University of Cambridge: 2020 Case Studies, 2020).

Most studies conducted in South Korea on the behaviour of piles due to tunnel construction have not considered pile

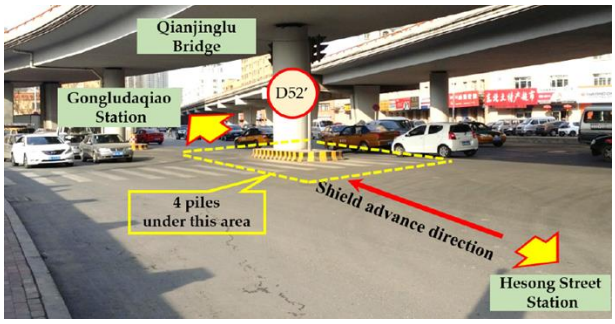

Fig. 2 Project planning area of the Harbin Metro Line 3 project (Wang and Yuan 2022)

cutting (damage) from tunnel excavation. Thus far, no studies have investigated the behaviour of piles after being directly cut during tunnel construction. According to Wang and Yuan (2022), cutting of existing reinforced concrete piles has been reported to occur often in TBM construction in China and Israel, with up to 14 piles having been cut during tunnel excavation in Israel. Fig. 2 depicts the project planning area wherein the Harbin Metro Line 3 passes must cut existing bridge piles, as presented by Wang and Yuan (2022). These examples highlight the need to investigate serviceability problems caused by pile cutting.

Therefore, in this study, we simulated the shield TBM method using a three-dimensional finite element analysis to study how pile tip cutting due to tunnel excavation affects pile behaviour. The effects of various reinforcement conditions on single and group piles were considered, focusing on tunnelling-induced pile head settlement, axial pile forces, relative displacement, and shear stress at the interface.

2. Numerical analysis

2.1 Overview and boundary conditions

The three-dimensional finite element analysis program Plaxis 3D (2024) was used to simulate tunnel excavation adjacent to single and group piles. Pile behaviour was analysed by considering various conditions, including pile tip cutting, grouting reinforcement, and pile cap reinforcement. Fig. 3(a) illustrates the representative finite element mesh applied in the analysis. The mesh sizes used in the model considered the element distribution to coarse mesh. Figs. 3(b) and 3(c) show the sectional and top views used in the analysis, respectively. In the finite element analysis, the tunnel diameter (D) was assumed to be 8 m, with the centre of the tunnel located 20.5 m below the surface. The ground was assumed to consist of a weathered soil layer up to 19 m from the surface, with a weathered rock layer underneath. The pile diameter (d) and pile length (L_p) were 0.5 and 20 m, respectively, simulating cast-in-situ piles, with a centre-to-centre spacing of 2.5d for the group piles. The analysis was performed by classifying the piles into single and group piles to examine pile behaviour. Pile tip cutting due to tunnel excavation was assumed to occur only in group piles. Therefore, the position of the single pile

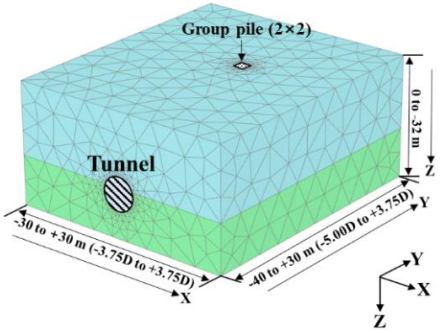

(a) Representative three-dimensional finite element mesh used in this study (2 × 2 pile group, D denotes tunnel diameter)

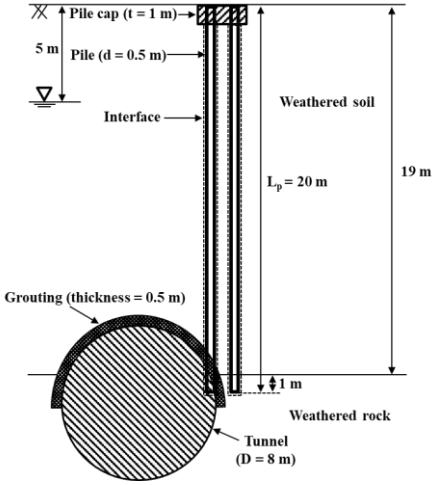

(b) Sectional view of the analysis geometry

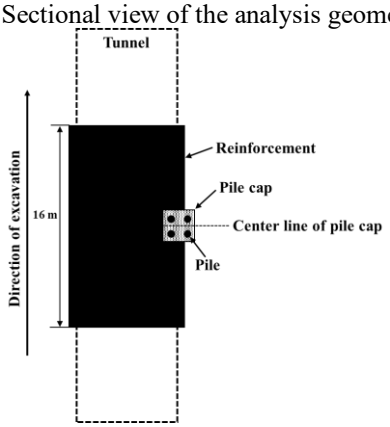

(c) Top view of the analysis geometry

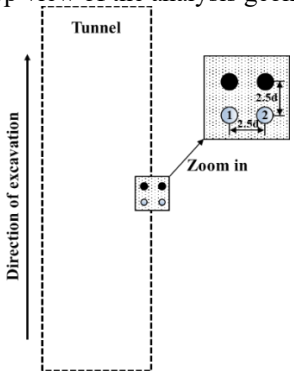

(d) Locations of the piles in the 2 × 2 pile group

Fig. 3 Structural elements used in analyses and their geometries

Table 1 Characteristics of the numerical analyses

Analysis	Ground Reinforcement Thickness	Pile Cap Reinforcement Thickness	Remarks
PL	-	-	Pile load test
Gr	-	-	Greenfield
S_p	-	-	Single pile without reinforcement
G_p	-	-	Pile group without reinforcement
G_p-G	0.5 m	-	Pile group with ground reinforcement
G_p-GC	0.5 m	1 m	Pile group with ground and pile cap reinforcements

Table 2 Pile locations and analysis conditions

Analysis	Ground Reinforcement	Pile Cap Reinforcement	Pile Location (shown in Fig. 3(d))	Remarks
S_p-2 (DL)	-	-	2	Design load condition
G_p-1 (DL)	-	-	1	
S_p-2	-	-	2	Single pile without pile cap or ground reinforcements
G_p-1	-	-	1	Pile group without pile cap or ground reinforcements
G_p-2	-	-	2	
G_p-G-1	Y	-	1	Pile group with ground reinforcement
G_p-G-2	Y	-	2	
G_p-GC-1	Y	Y	1	Pile group with pile cap and ground reinforcements
G_p-GC-2	Y	Y	2	

was selected as position 2 in the group pile condition (Fig. 3(d)). Prior to tunnel construction below the piles, the pile tips were assumed to be embedded 1 m into the weathered rock for all pile conditions. In the group pile analysis, certain pile tips in contact with the tunnel were cut owing to tunnel excavation. Thus, grouting reinforcement or pile cap reinforcement was performed before the construction of the tunnel below the piles. The grouting reinforcement had a fixed angle of 180° and a thickness of 0.5 m. For the grouting reinforcement, 2 m reinforcements were applied at the initial and final reinforcement points and 1.5 m reinforcements were applied in the remaining areas. The grouting reinforcement was considered simultaneously with the pile cap reinforcement (t), which was applied at the initial grouting reinforcement point (explained in Section 2.3). Through back analysis, the face pressure of the tunnel was determined to be the minimum face pressure preventing ground collapse due to tunnel excavation, that is, 180 kPa and assumed to act uniformly on the tunnel face. Table 1 summarises the characteristics of each analysis conducted in this study (a total of six analyses were conducted). For the group pile analysis, piles with cut tips (Pile 1) and without cut tips (Pile 2) were analysed and considered. Their positions are shown in Fig. 3(d). Table 2 presents the pile locations and reinforcement conditions. In this analysis, the groundwater level was assumed to be 5 m below the surface, and during tunnel excavation, the tunnel interior was assumed to be free of groundwater.

2.2 Applied constitutive models and material properties

An elastoplastic analysis was performed to simulate tunnel excavation, and an interface element was applied to allow slip to occur in the case of plastic yielding at the boundary between the ground and the pile. The aim was to analyse the transfer process of shear stress at the boundary between the pile and the adjacent ground. To ensure the pile tip and ground could separate when tensile forces acted on the pile, an interface element was specified at the pile tip. Table 3 lists the material and ground properties applied in the numerical analysis. These properties are typical of weathered soil, weathered rock, and concrete in South Korea (Lee 2012a). The grouting material properties were obtained using the method presented by Choi *et al*. (2003) through back analysis, and the properties applied to the pile were also used for the pile cap. An elastoplastic model based on the non-associated flow rule and Mohr–Coulomb failure criterion was applied to the weathered soil and rock, and an isotropic elastic model was assigned to the pile cap, pile, and segments. To consider the reduction in shear strength constants (c'_{int}, φ'_{int}) at the pile shaft–ground and pile tip–ground interfaces due to pile construction, a strength reduction factor, R_{int} = 0.75, was applied according to the guidelines set out by Brinkgreve *et al*. (2015). The appropriate shear strength constants were then calculated using Eqs. (1) and (2), as expressed below.

Table 3 Material and ground parameters for numerical modelling

Material	Model	γ_t (kN/m^3)	K_0	ν'	E' (MPa)	c' (kPa)	$\emptyset'$ (°)
Weathered soil (Lee 2012a)	Mohr–Coulomb	20	0.75	0.35	80	50	35
Weathered rock (Lee 2012a)	Mohr–Coulomb	20	0.75	0.25	200	100	35
Grouted material (Choi *et al.* 2003)	Mohr–Coulomb	25	0.01	0.2	800	250	35
Shield TBM machine (Plaxis 3D 2024)	Elastic	247	-	-	200,000	-	-
Segment (Plaxis 3D 2024)		27	0.01	0.1	31,000	-	-
Pile/Pile cap		25	0.01	0.2	30,000	-	-

Note: γ_t (unit weight of material), K_0 (lateral earth pressure coefficient at rest), ν' (Poisson's ratio), E' (Young's modulus), c' (cohesion), and $\emptyset'$ (internal friction angle)

$$c'_{int} = R_{int} \times c'_{soil}, \quad (1)$$

$$tan(\varphi'_{int}) = R_{int} \times tan(\varphi'_{soil}), \quad (2)$$

where c'_{soil} is the cohesion of the ground, R_{int} is the strength reduction factor, φ'_{soil} is the internal friction angle of the ground, and φ'_{int} is the interface friction angle (calculated as 27.7°).

2.3 Numerical analysis process and examination

The change in ground stress due to pile installation was not included in the numerical analysis; thus, the piles in this study were considered similar to cast-in-situ piles. Tunnel excavation was conducted in the range of −5.00D to +3.75D (−40 m to +30 m) in the longitudinal direction (Y) (Fig. 3(a)). Before implementing step-by-step tunnel excavation, the design load (P_a = 1,800 kN) determined through a separate analysis was applied, and the load on the pile head was gradually increased in stages (600 kN → 1,200 kN → 1,800 kN). A tunnel excavation 19 m in length was assumed to have been completed, with the shield TBM equipment having a length of 9 m within the 19 m excavation. The step-by-step tunnel excavation was executed in 34 steps, advancing 1.5 m per step. The cutting of pile tips due to tunnel excavation was simulated by cutting the overlapping portion of the tunnel's cross-section and pile tip, as illustrated in Fig. 3(b), assuming that approximately 1 m of the pile tip was cut. Grouting reinforcement was executed in the longitudinal direction (Y) ±1D (±8 m, 16 m reinforcement in total) from the centreline of the pile cap (Fig. 3(c)). At the initial and final reinforcement points, 2 m of reinforcement was applied, while in the remaining reinforcement areas, 8 rounds of reinforcement corresponding to the tunnel excavation length (1.5 m) were applied (18 m reinforcement: initial reinforcement (2.0 m) → [excavation (1.5 m) → reinforcement (1.5 m)] × 8 times → excavation (1.5 m) → final reinforcement (2.0 m)). Additionally, in the analysis considering both pile cap and grouting reinforcements, the pile cap reinforcement was applied when the grouting reinforcement commenced. As explained in Section 2.1, the face pressure of the tunnel was determined using back analysis to be the minimum face pressure preventing ground collapse due to tunnel excavation and uniformly applied to the tunnel face. For the analysis, the pile axial force P at a given depth was calculated using the formula $P = \sigma_{zz,avg} \times A_p$, where $\sigma_{zz,avg}$ is the average vertical stress of the pile at a specific depth, and A_p is the cross-sectional area of the pile.

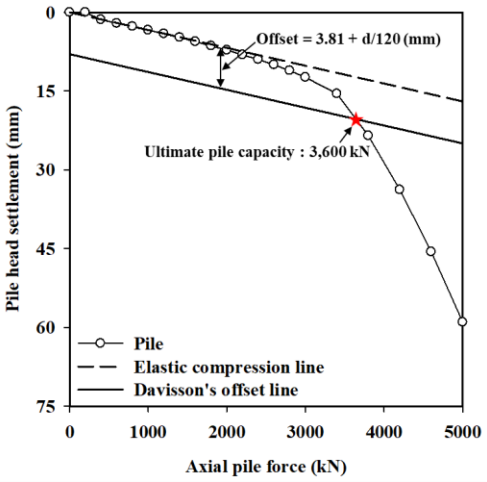

Fig. 4 Relationship between the axial pile forces and pile head settlements

3. Results and discussion

3.1 Determination of the design pile bearing capacity

Fig. 4 illustrates the load–settlement relationship of the pile calculated through a simulated pile load test. This relationship was used to determine the design bearing capacity of the piles. Tunnel excavation was not included in the calculation of the design bearing capacity of the piles, and the load test was simulated by gradually increasing the compressive load on the pile head. Fig. 4 illustrates that the relationship between the pile load and pile head settlement is almost linear until the pile head load reaches

approximately 3,100 kN; beyond this, rapid settlement occurs. In this study, the widely used method proposed by Davisson (1972) was applied to determine the designed bearing capacity of the piles from the load–settlement relationship. The estimated pile failure load was 3,600 kN. By applying a safety factor (Fs) of 2.0, we calculated the design load (P_a) to be 1,800 kN (3,600 kN/2 = 1,800 kN). The settlement (△) of the pile head under the applied design load (P_a) was 5.6 mm. To analyse the behaviour of a pre-installed pile during the excavation of the boundary between the pile and ground, we applied the load to the head of the pile in three stages (600 kN → 1,200 kN → 1,800 kN). The load was applied before tunnel excavation to simulate the design load (P_a). This process simulated the behaviour of the piles in use, after which the tunnel excavation was performed step-by-step.

3.2 Settlement of pile heads and the ground surface due to tunnel excavation

Fig. 5 illustrates the distribution of normalised settlements ($\triangle_{p,n}/\triangle_{g,max}$ and $\triangle_g/\triangle_{g,max}$) at each stage of tunnel excavation for single and group piles, considering various reinforcement conditions (Y/D: normalised longitudinal direction). Here, $\triangle_g$ represents the ground surface settlement at each stage of tunnel excavation at position 1 of the group pile under greenfield conditions without piles or reinforcement. $\triangle_{p,n}$ purely represents the pile head settlement at each stage of tunnel excavation. Additionally, $\triangle_{g,max}$ is the maximum ground surface settlement due to tunnel excavation under greenfield conditions ($\triangle_{g,max}$ = 5.56 mm). As shown in Fig. 5, the normalised settlements, $\triangle_{p,n}/\triangle_{g,max}$ and $\triangle_g/\triangle_{g,max}$, gradually increase as the excavation stages progress. The highest ratios of the pile head and ground surface settlements occurred when the tunnel passed through the Y/D = −1.5 to +1.5 zone. Thereafter, the settlement ratios significantly decreased. Thus, the pile head settlement due to tunnel excavation mainly occurred when the tunnel passed through the Y/D = −1.7 to +1.7 zone. The final settlement of the pile heads exceeded that of the ground surface under greenfield conditions for all piles, except the G_p-G-2 pile. Moreover, before the tunnel passed directly under the piles (Y/D = 0), the settlement of all piles was less than that of the ground surface under greenfield conditions. Additionally, for all piles, the pile head settlement gradually increased until the tunnel reached the Y/D = 0 point, after which it decreased.

This phenomenon was caused by the segment installation effect and stress concentration occurrence in the simulation of the shield TBM excavation method. The G_p-G-2 pile experienced the smallest settlement at the pile head, which was attributed to the pile tip being supported by weathered rock and the effective reinforcement from grouting. Additionally, the G_p-GC-2 pile, which considered both pile cap and grouting reinforcements, demonstrated a larger settlement than that of the G_p-G-2 pile because the weight of the pile cap connected to the pile head affected the pile. In contrast, for the G_p-G-1 and G_p-GC-1 piles, where the pile tip was cut, the pile head settlement in G_p-GC-1 was reduced compared to that in G_p-G-1 because of

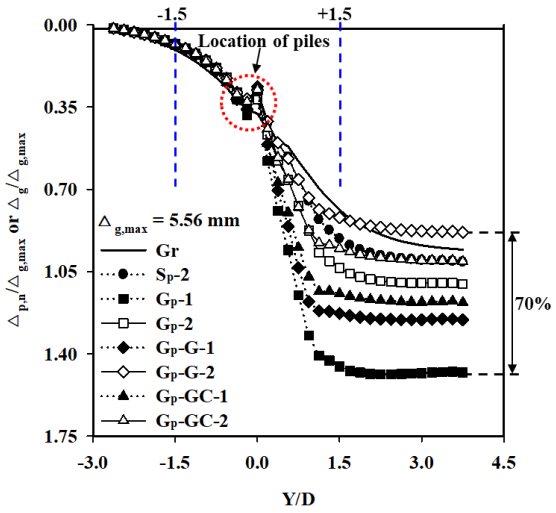

Fig. 5 Normalised pile head and soil surface settlement with tunnel advancement ($\triangle_{gr,max}$ = 5.56 mm)

the effective application of pile cap reinforcement. Therefore, the presence or absence of support at the pile tip resulted in different magnitudes of settlement, and the reinforcement effect of the pile cap also varied. Additionally, the final settlement of the G_p-1 pile was approximately 70% greater than that of the G_p-G-2 pile, which experienced the smallest settlement. Upon analysing the settlement pattern, we predicted that differential settlement could occur in the pile cap as the settlement magnitudes differed for piles located at positions 1 and 2 in the group pile connected to the pile cap.

3.3 Lateral displacement of piles and ground

Fig. 6 illustrates the normalised lateral displacements, $\triangle x_p/\triangle x_{g,max}$ and $\triangle x_g/\triangle x_{g,max}$, after tunnel excavation for single and group piles, considering various reinforcement conditions along the normalised pile depth (Z/L_p). Here, $\triangle x_g$ represents the lateral displacement at each group pile depth at position 1 under greenfield conditions without piles or reinforcement. $\triangle x_p$ represents the lateral displacement of the pile calculated after tunnel excavation. Additionally, $\triangle x_{g,max}$ is the maximum lateral displacement at the group pile depth at position 1 under greenfield conditions ($\triangle x_{g,max}$ = 6.93 mm). Fig. 6 illustrates that the piles without reinforcement, that is, S_p-2, G_p-1, and G_p-2, experience displacements exceeding those under greenfield conditions for most of the pile depth. This phenomenon indicates that the pile displacement is greater than the ground displacement, thus necessitating appropriate reinforcement. Additionally, for piles at position 2, with the pile tip supported by weathered rock, the displacement was significantly restrained near the pile tip. The lateral displacement of the pile demonstrated a different pattern from that of the vertical settlement, with the piles that had applied reinforcement exhibiting a displacement below that under greenfield conditions. Thus, the grouting and pile cap reinforcements effectively restrained the lateral

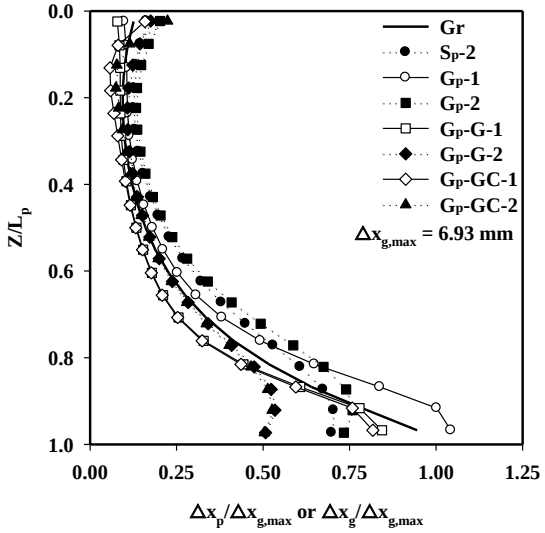

Fig. 6 Normalised lateral displacement with depth ($\triangle x_{gr,max}$ = 6.93 mm)

displacement caused by tunnel excavation. Therefore, the largest lateral displacement occurred for the G_p-1 pile with no reinforcement and a cut pile tip, suggesting potential serviceability problems.

3.4 Moment distribution in piles due to tunnel excavation

Figs. 7(a) and 7(b) illustrate the distribution of the lateral (M_{xx}) and longitudinal (M_{yy}) bending moments induced in the piles, respectively, due to tunnel excavation, considering various reinforcement conditions along the normalised pile depth (Z/L_p). The magnitude of the bending moments was calculated using the formulas M_{xx} = EI × $(\frac{d^2f(x)}{dz^2})$ and M_{yy} = EI×$(\frac{d^2f(y)}{dz^2})$, where f(x) and f(y) are the lateral and longitudinal forces, respectively, obtained from a numerical analysis of the pile's centre. Here, E is the pile's modulus of elasticity, I is the moment of inertia, and dz is the vertical distance between two nodes. Figs. 7(a) and 7(b) illustrate that the lateral displacement of the pile is generally far greater than the longitudinal displacement, resulting in M_{xx} being larger than M_{yy}. Fig. 7(a) demonstrates that the largest bending moment occurs at position 1, where the pile tip is cut, with a maximum bending moment of approximately −90 kNm occurring in the G_p-1 pile. Additionally, the G_p-GC-1 and G_p-GC-2 piles reinforced by a pile cap exhibited relatively larger bending moments near the pile head than the other piles because of the resistance generated by the pile cap. Fig. 7(b) illustrates the M_{yy} bending moments, which are, as expected, much smaller than the M_{xx} bending moments. Similar to the M_{xx} bending moments, the largest bending moment occurred near the pile tip at position 1 where the pile tip was cut. The value was calculated to be approximately −5 kNm. If we assume that the allowable bending strength of concrete is 7.5 MPa, the allowable bending moment of the pile is 92.0

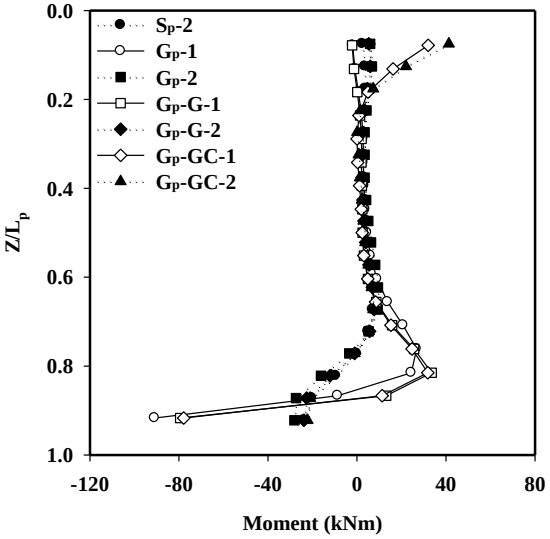

(a) Bending moment M_{xx} with depth

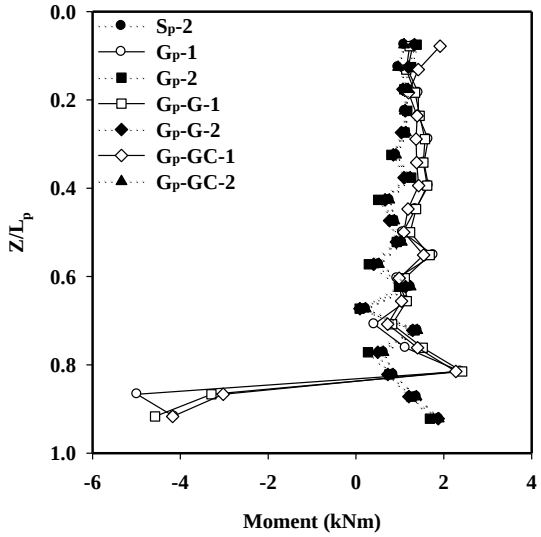

(b) Bending moment M_{yy} with depth

Fig. 7 Bending moments in the piles

kNm, which is approximately 102.2% that of the previously calculated maximum bending moment (−90 kNm). This result indicates that the lateral displacement of the pile caused by tunnel excavation can potentially cause severe issues pertaining to the serviceability of the piles.

3.5 Settlement of pile heads and the ground surface with volume loss

Fig. 8 illustrates the normalised tunnelling-induced pile head settlements ($\triangle_{p,n}/\triangle_{g,max}$) and greenfield ground surface settlements ($\triangle_g/\triangle_{g,max}$) at Y/D = 0 for single and group piles, considering various reinforcement conditions with respect to tunnelling-induced volume loss. Here, $\triangle_g$ represents the ground surface settlement at each stage of

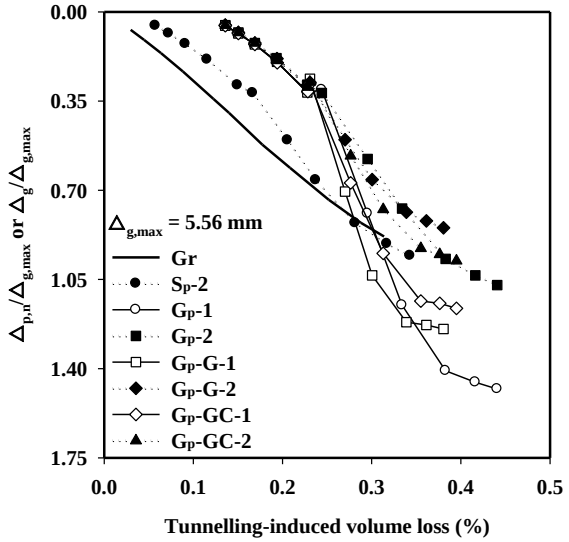

Fig. 8 Normalised tunnelling-induced pile head and greenfield soil surface settlements with tunnelling-induced volume loss at Y/D = 0

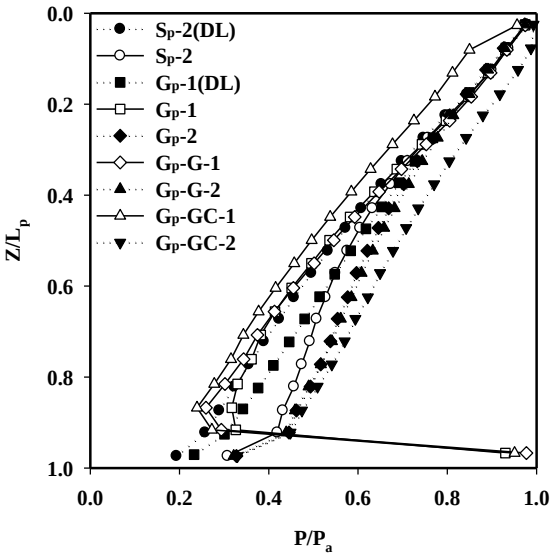

Fig. 9 Normalised axial pile forces with depth

tunnel excavation at position 1 of the group pile under greenfield conditions without piles or reinforcement. For the pile at position 1, where the pile tip was cut, the settlements were smaller than those of the greenfield ground surface until the volume loss reached approximately 0.29%. As the volume loss increased beyond this value, the pile settlements exceeded those of the greenfield ground surface. However, for the pile at position 2 with the tip supported by weathered rock, except for the S_p-2 pile, the pile settlements did not exceed the greenfield settlements up to the maximum volume loss. This phenomenon is attributed to the supporting effects of the pile tip and reinforcement. Consequently, the conditions without reinforcement and pile support demonstrated increased volume loss and pile settlement compared to the conditions with reinforcement and pile support. Macklin (1999) analysed and reported on various volume losses in over-consolidated clay ground due to tunnelling in the UK, revealing a volume loss range of approximately 0.5% to 3.0%. In contrast, insufficient theoretical studies and measured data on volume loss are available in South Korea. Utilising volume loss considerations for construction management, ground settlement prediction, and structural stability assessment in South Korea will be necessary in the near future.

3.6 Axial force distribution in piles

Fig. 9 illustrates the distribution of normalised axial forces (P/P_a) in single and group piles with various reinforcement conditions after tunnel excavation along the normalised pile depth (Z/L_p). The figure also illustrates the distribution of axial forces for the design load applied to the pile head before tunnel excavation. Here, P represents the axial force at any depth, and P_a is the design load (1,800 kN) applied to the pile head before tunnel excavation. As mentioned in Section 2.3, the axial pile force is calculated by averaging the vertical stress at any depth. For S_p-2 (DL) and G_p-1 (DL), with only the design load applied, the axial pile force gradually decreased with depth, with approximately 80% supported by shaft friction and the remaining 20% by the pile tip. After tunnel excavation, for the S_p-2, G_p-2, G_p-G-2, and G_p-GC-2 piles with pile tips supported by weathered rock, approximately 70% of the load was supported by shaft friction and the remaining 30% by the pile tip. This result is attributed to the significant resistance at the pile tip caused by settlement due to tunnel excavation. In contrast, for the G_p-1, G_p-G-1, and G_p-GC-1 piles where the pile tip was cut due to tunnel excavation, the axial pile force gradually decreased until a Z/L_p of approximately 0.85 from the surface was reached. The force then increased again, with an axial pile force close to the design load occurring at the pile tip. This is attributed to stress changes due to segment installation and grouting reinforcement immediately after pile tip cutting, suggesting that tip resistance was restored after initially being relieved. However, because isolating the axial pile force distribution caused by tunnel excavation from the total distribution is difficult, examining the distribution of the axial pile force induced purely by tunnel excavation is necessary.

Fig. 10 illustrates the distribution of normalised tunnelling-induced axial pile forces (P_n/P_a) in single and group piles with various reinforcement conditions along the normalised pile depth (Z/L_p). These distributions were used to clearly identify the changes in axial pile forces due to tunnel excavation. Here, P_n represents the axial pile force caused purely by tunnel excavation. Fig. 10 illustrates that for all piles at position 2 with pile tips supported by weathered rock, the axial pile force gradually increases from the surface to approximately Z/L_p = 0.9 owing to tunnel excavation and then subsequently decreases towards the pile tip. In contrast, for all piles at position 1 where the pile tip was cut due to tunnel excavation, the axial pile force gradually decreased from the surface to approximately Z/L_p

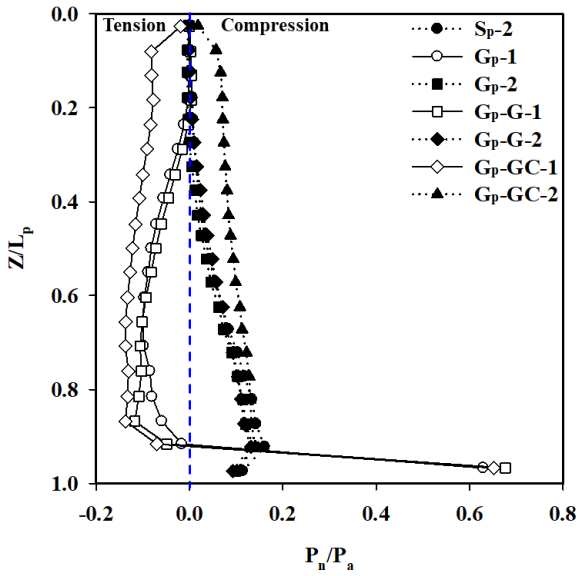

Fig. 10 Normalised tunnelling-induced axial pile forces with depth

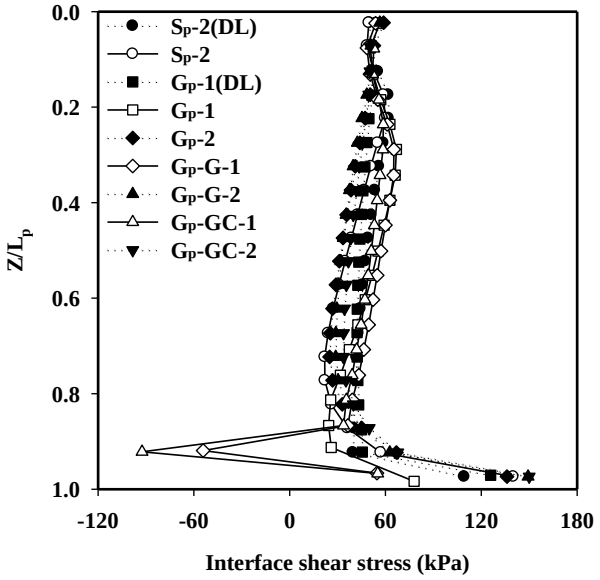

Fig. 11 Interface shear stresses with depth

= 0.9 and then significantly increased from Z/L_p = 0.9 to the pile tip. This occurred because the cutting of the pile tip and release of ground stress at position 1 due to tunnel excavation, followed by segment installation and grouting reinforcement effects caused a stress concentration. Additionally, the piles at positions 1 and 2 exhibited different axial pile force distributions, with compression forces at position 2 due to the pile tip being supported by weathered rock. At position 1, where the pile tip was cut, tensile forces were observed from the surface to approximately Z/L_p = 0.9, after which compression forces were observed towards the pile tip. The mechanisms of the compression and tensile forces acting on the pile are explained in detail in Section 3.8 with regard to the relative displacement distribution of the pile. For the G_p-GC-1 and G_p-GC-2 piles, with both grouting and pile cap reinforcements, the axial pile forces in both tension and compression were larger than those of the other piles because of the combined effects of grouting and pile cap reinforcements, as well as the added weight of the pile cap.

3.7 Shear stress distribution of piles

Fig. 11 illustrates the distribution of shear stress at the pile–ground interface after tunnel excavation for single and group piles, considering various reinforcement conditions along the normalised pile depth (Z/L_p). The figure also illustrates the shear stress distribution before tunnel excavation and after applying the design load. The shear stress distribution of the S_p-2 (DL) and G_p-1 (DL) piles with the design load applied before tunnel excavation demonstrated similar trends. However, slight differences in the values emerged because of the group effect in group piles. For the G_p-1, G_p-G-1, and G_p-GC-1 piles, where pile tip cutting occurred owing to tunnel excavation, the shear stress increased from the surface to approximately Z/L_p = 0.3, decreased to Z/L_p = 0.9, and increased again towards the pile tip. Additionally, the G_p-G-1 and G_p-GC-1 piles showed negative shear stress values around Z/L_p = 0.9, which was attributed to stress concentration effects due to grouting reinforcement and segment installation. For all piles at position 2 with pile tips supported by weathered rock, the shear stress decreased from the surface to approximately Z/L_p = 0.75 and then increased towards the pile tip. When the pile tip was supported by weathered rock, the shear stress distribution was similar to that under the design load condition, thus minimising the impact of tunnel excavation on the pile and surrounding ground.

Fig. 12 illustrates the distribution of shear stress caused purely by tunnelling for single and group piles with various reinforcement conditions along the normalised pile depth (Z/L_p). As illustrated in the figure, all piles with pile tips supported by weathered rock exhibit similar trends in the distribution of shear stress caused purely by tunnelling. Additionally, for all piles at position 2, the direction of shear force acting on the pile was reversed at approximately Z/L_p = 0.87. This indicates that from the surface to Z/L_p = 0.87, the downward shear stress was caused by ground settlement exceeding pile settlement. Meanwhile, from Z/L_p = 0.87 to the pile tip, the upward shear stress was caused by pile settlement exceeding ground settlement, resulting in a compression force distribution in the pile. In contrast, for the G_p-1, G_p-G-1, and G_p-GC-1 piles, the shear stress value was close to zero from the surface to approximately Z/L_p = 0.17, increased to approximately Z/L_p = 0.7, and then decreased and became negative beyond Z/L_p = 0.7. Additionally, the positive shear stress reappeared at the tip, demonstrating both compression and tensile force distributions throughout the pile. The upward shear stress for piles at position 1 was observed from Z/L_p = 0.17 to Z/L_p = 0.70 because the pile settlement was greater than the ground settlement. This outcome was followed by the

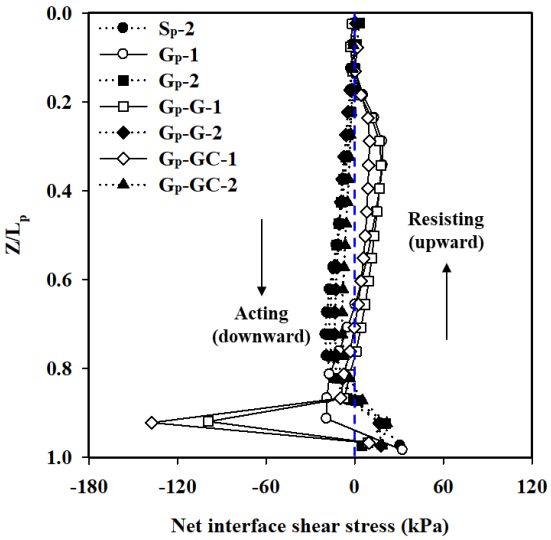

Fig. 12 Tunnelling-induced interface shear stresses with depth

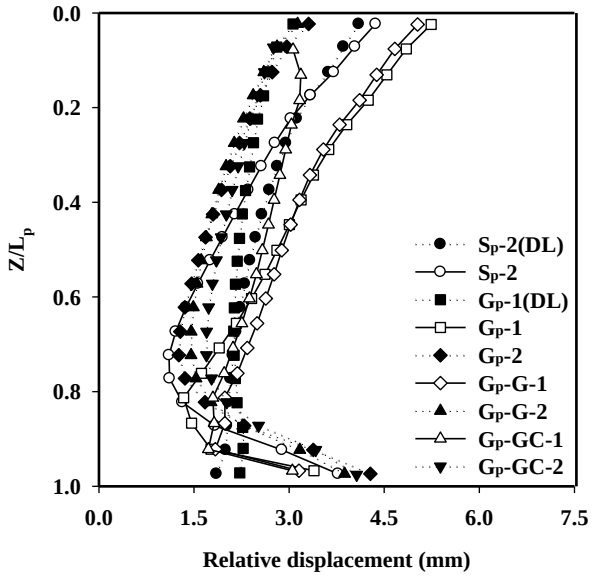

Fig. 13 Relative displacement with depth

downward shear stress below this range, demonstrating a tensile force distribution. The shear direction changed again near the pile tip, indicating both tensile and compression forces throughout the pile depth. Particularly for the G_p-G-1 and G_p-GC-1 piles, significant shear stress was calculated near the pile tip. This significant stress is attributed to the support from grouting reinforcement and segment installation, which restrained pile settlement, resulting in a compression force distribution.

3.8 Relative displacement distribution in piles

Fig. 13 illustrates the distribution of relative displacement at the pile–ground interface calculated for single and group piles with various reinforcement conditions due to tunnel excavation along the normalised pile depth (Z/L_p). Owing to the design load applied to the pile head before tunnel excavation, the settlement of the pile exceeded that of the ground over the entire pile length. The relative displacement distribution of the pile under the design load demonstrated similar trends for both single and group piles, but the relative displacement of the entire pile was smaller for group piles than for single piles. This result is attributed to the group effect, where the surrounding grounds tend to move together because of overlapping effects from pile settlement. Additionally, the relative displacement distribution of all piles calculated after tunnel excavation decreased from the pile head to approximately $Z/L_p = 0.8$ and then increased towards the pile tip. For the pile at position 1, where the pile tip was cut due to tunnel excavation, the relative displacement after tunnel excavation was larger than that of the piles supported by weathered rock. This result indicates that pile tip cutting can affect pile serviceability. For the G_p-GC-1 pile, the relative displacement significantly decreased because of the grouting and pile cap reinforcements, indicating the

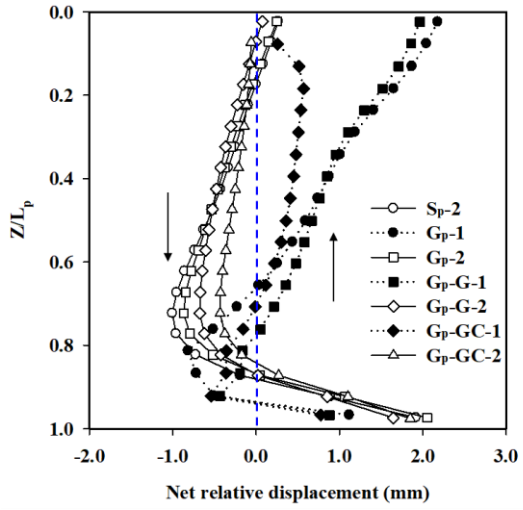

Fig. 14 Tunnelling-induced relative displacement at the pile–soil interface with depth

appropriate application of reinforcement effects. Therefore, the trend of the changes in relative displacement varies depending on whether the pile tip is cut, and various reinforcement conditions can be applied, necessitating a detailed examination of the tunnelling-induced relative displacement.

Fig. 14 illustrates the distribution of tunnelling-induced relative displacement for single and group piles, considering various reinforcement conditions along the normalised pile depth (Z/L_p). For the G_p-1 and G_p-G-1 piles, the relative displacement was larger than that of the other piles, with the largest relative displacement occurring in the unreinforced G_p-1 pile. Additionally, the G_p-GC-1 pile, which was

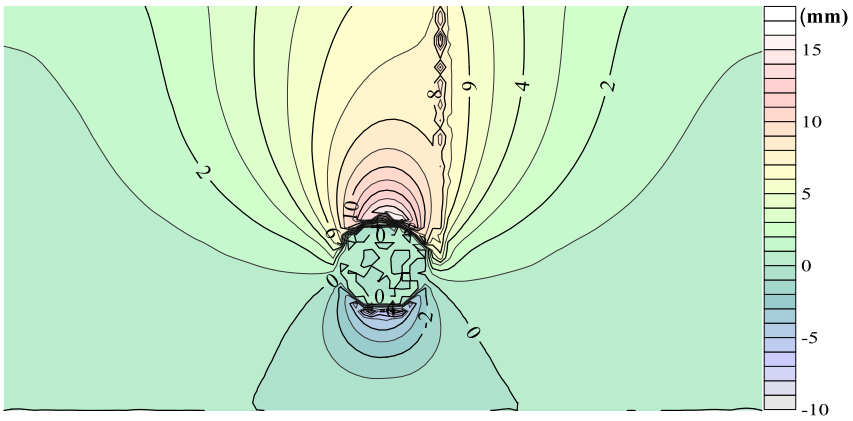

(a) S_p condition

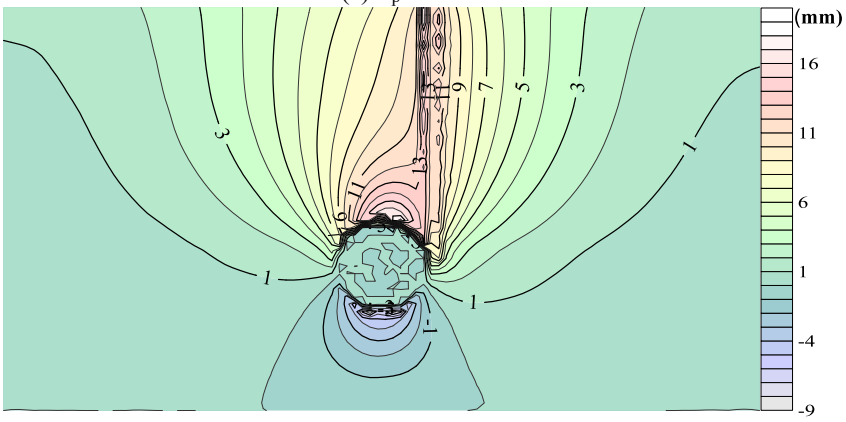

(b) G_p condition

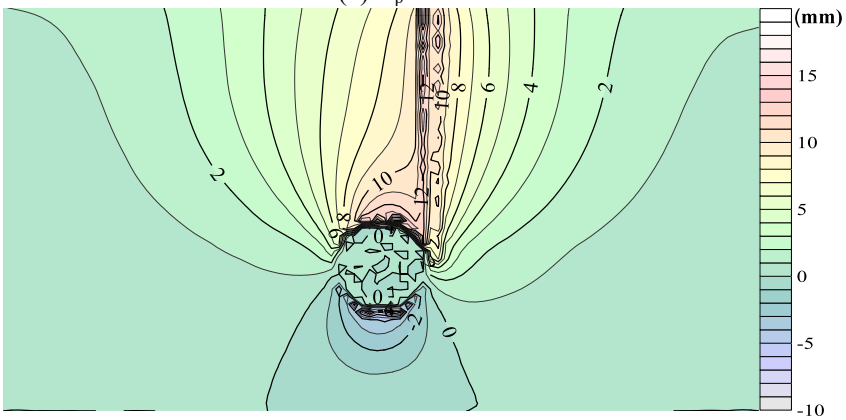

(c) G_p-G condition

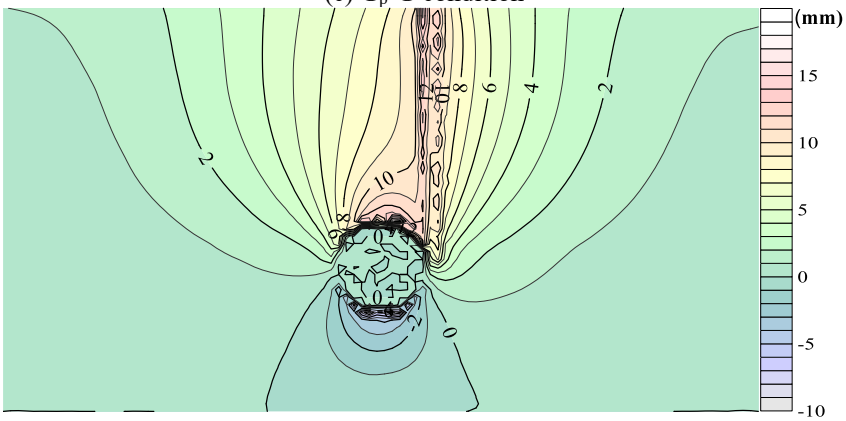

(d) G_p-GC condition

Fig. 15 Vertical displacement contours of the pile and surrounding ground (X–Z plane)

reinforced by grouting and a pile cap, showed the smallest relative displacement among the piles at position 1, proving the appropriate effectiveness of the reinforcement. For the G_p-1, G_p-G-1, and G_p-GC-1 piles, the relative displacement value turned negative at approximately Z/L_p = 0.75 and turned positive again at approximately Z/L_p = 0.9. This behaviour indicates that the direction of friction changed twice along the pile length. Thus, both compressive and tensile axial forces occurred in the pile. For piles supported by weathered rock, the relative displacement decreased from the surface to approximately Z/L_p = 0.7, then increased with a sign change at approximately Z/L_p = 0.85. This phenomenon indicates that downward friction acts on the upper part of the pile because of ground settlement, whereas upward friction acts on the lower part of the pile because of the ground resisting pile settlement. Therefore, the distribution of axial and shear stresses previously explained is reconfirmed by tunnelling-induced relative displacement. Pile tip cutting due to tunnel excavation increases the relative displacement between the pile and the ground and can be reduced with appropriate reinforcement.

3.9 Distribution of pile and ground settlements with various reinforcement conditions (contour and displacement vectors)

Figs. 15(a)-15(d) illustrate the contour of settlements for piles and the ground after tunnel excavation, considering various reinforcement conditions for single and group piles at the pile location on the X–Z plane. Fig. 15(a) illustrates the vertical displacement contours of the piles and ground caused by tunnel excavation under the S_p condition. The settlement of the pile head under the S_p condition exceeds the ground settlement, with the opposite trend occurring as the pile depth increases. Fig. 15(b) illustrates the group pile under the G_p condition without reinforcement, where the settlement of Pile 1, whose tip is cut, is larger than that of Pile 2, whose tip is supported. Additionally, owing to the group effect of the piles, the ground settlement around the group piles is greater than that around a single pile. Figs. 15(c) and 15(d) illustrate the vertical displacement contours under the G_p-G and G_p-GC conditions, respectively. The different settlements of Piles 1 and 2 under these conditions indicate potential differential settlement for piles connected by a pile cap under the G_p-GC condition. Additionally, the pile head and pile tip near the cut pile tip experienced settlements exceeding the ground settlement, creating pulling effects in opposite directions on the pile, delineating the previously mentioned tensile force mechanism.

Figs. 16(a)-16(d) illustrate the displacement vectors after tunnel excavation for single and group piles, considering various reinforcement conditions at the pile location on the X–Z plane. Figs. 16(a) and 16(b) illustrate the displacement vectors under conditions without reinforcement, with a larger vector distribution and magnitude under the G_p condition compared to the S_p condition. Additionally, the magnitude of the displacement vectors in the ground around the tunnel is larger for the S_p and G_p conditions than the G_p-G and G_p-GC conditions, where grouting reinforcement is considered. The distribution of displacement vectors due to tunnel excavation is similar to the influence zone of the tunnel excavation, as presented by Jacobsz (2002), because the pile tip is within the influence zone, thus pile serviceability can be affected.

4. Conclusions

A three-dimensional finite element analysis was used to simulate shield TBM tunnel excavation adjacent to single and group piles, considering various conditions such as pile tip cutting, grouting reinforcement near the tunnel, and pile cap reinforcement. The analysis examined tunnel-induced pile settlement, axial force, shear stress, relative displacement, and ground displacement around the tunnel. The following conclusions can be drawn from the results obtained.

1. The highest pile head and ground surface settlement ratios occurred when the tunnel passed through the Y/D = −1.5 to +1.5 zone, after which the settlement ratios significantly decreased. The final pile head settlement exceeded the greenfield condition's final ground surface settlement for all piles, except the G_p-G-2 pile. Before the tunnel passed directly beneath the piles (Y/D = 0), all piles demonstrated less pile head settlement than the greenfield condition's ground surface settlement. Additionally, the difference between the maximum and minimum pile head settlements after tunnel excavation was approximately 70% greater than the minimum settlement.
2. The analysis of the lateral displacement of the piles showed that piles with tips supported by weathered rock had significantly restrained displacement near the pile tip. The lateral displacement of the piles exhibited different patterns from those owing to vertical settlement, with reinforced piles showing a smaller lateral displacement than under greenfield conditions. In other words, grouting and pile cap reinforcements effectively restrained the lateral displacement caused by tunnel excavation. Owing to the lateral displacement of the piles, M_{xx} bending moments occurred, with the maximum bending moment reaching approximately 97.8% of the allowable bending moment, indicating potential serviceability problems for the pile.
3. For piles with cut tips due to tunnel excavation, the axial force gradually decreased from the surface to approximately Z/L_p = 0.85 and then increased towards the pile tip. Axial forces near the design load occurred at the pile tip. This phenomenon was attributed to the stress changes from the segment installation and grouting reinforcement immediately after the pile tip was cut, suggesting that tip resistance was restored after initially being relieved.
4. Pile tip cutting due to tunnel excavation resulted in two changes in the shear force direction along

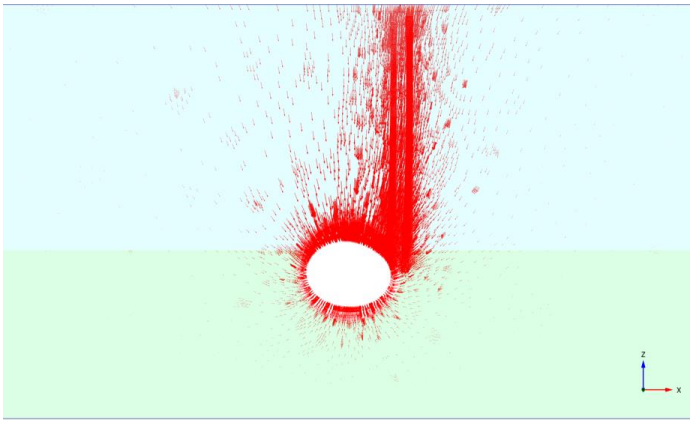

(a) S_p condition

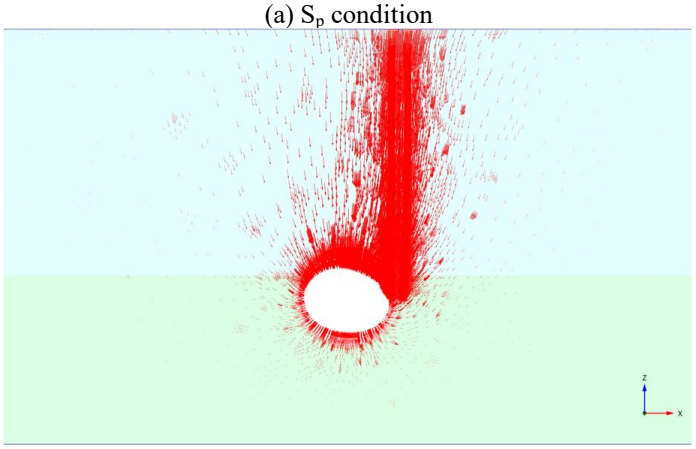

(b) G_p condition

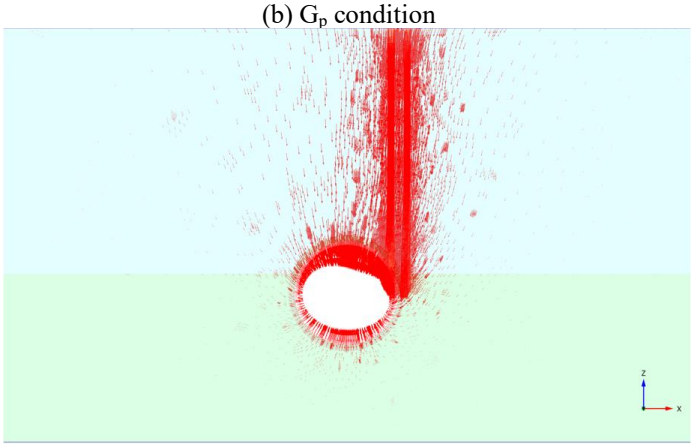

(c) G_p-G condition

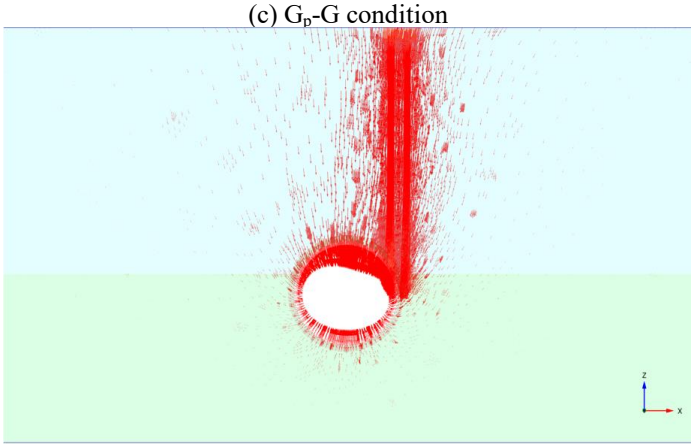

(d) G_p-GC condition

Fig. 16 Displacement vector plots around the tunnel and pile (X–Z plane)

the entire pile length, indicating both compressive and tensile axial force distributions. Upward shear forces occurred in the range of Z/L_p = 0.17 to Z/L_p = 0.70 because the pile settlement exceeded the ground settlement, followed by downward shear forces below this range, indicating tensile axial forces, with compressive forces occurring near the pile tip. A comprehensive analysis showed that the behaviour of piles due to tunnel excavation varied significantly depending on the reinforcement and pile conditions. Therefore, a thorough examination of the reinforcement effects on the ground adjacent to piles and tunnels is necessary as part of the continuing research on this issue in the future.

Acknowledgements

The research in this paper was supported by the National Research Foundation of Korea grant funded by the Korea government (MSIT) (RS-2023-00278033) and the Basic Science Research Program through the National Research Foundation of Korea funded by the Ministry of Education (2022R1A6A3A01085973).

References

Brinkgreve, R.B.J., Kumarswamy, S. and Swolfs, W.M. (2015), "Reference manual", *Plaxis 3D 2015 user's manual*, Delft, 1-284.

Cheng, C.Y., Dasari, G.R., Chow, Y.K. and Leung, C.F. (2007), "Finite element analysis of tunnel-soil-pile interaction using displacement controlled model", *Tunn. Undergr. Sp. Tech.*, **22**(4), 450-466. https://doi.org/10.1016/j.tust.2006.08.002.

Choi, Y.G., Park, J.H., Woo, S.B. and Jeong, Y.J. (2003), "Reinforcing effect of FRP multi-step grouting for NATM tunnel through weathered zone", *KSCE 2003 convention program*, Seoul, Korea.

Davisson, M.T. (1972), "High capacity piles", *Proceedings of Lecture Series in Innovations in Foundation Construction*, ASCE, Illinois Section.

Dias, T.G.S. and Bezuijen, A. (2014a), "Pile tunnel interaction: Literature review and data analysis", *ITA World Tunnel Congress 2014*, Iguassu Falls, Brazil, May.

Dias, T.G.S. and Bezuijen, A. (2014b), "Pile-tunnel interaction: A conceptual analysis", *Proceedings of the 8th International Symposium on Geotechnical Aspects of Underground Construction in Soft Ground*, CRC Press, Seoul, Korea, August.

Hartono, E., Leung, C.F., Shen, R.F., Chow, Y.K., Ng, Y.S., Tan, H.T. and Hua, C.J. (2014), "Behaviour of pile above tunnel in clay", *Proceedings of the 8th International Conference on Physical Modelling in Geotechnics*, Perth, Australia, January.

Hong, Y., Soomro, M.A. and Ng, C.W.W. (2015), "Settlement and load transfer mechanism of pile group due to side-by-side twin tunnelling", *Comput. Geotech.*, **64**, 105-119. https://doi.org/10.1016/j.compgeo.2014.10.007.

Jacobsz, S.W. (2002), "The effects of tunnelling on piled foundations", Ph.D. Thesis, University of Cambridge, Cambridge, U.K.

Jeon, Y.J. and Lee, C.J. (2015), "A study on the behaviour of single piles to adjacent tunnelling in stiff clay", *J. Korean Geo-Environ. Soc.*, **16**(6), 13-22. https://doi.org/10.14481/jkges.2015.16.6.13.

Jeon, Y.J., Kim, S.H. and Lee, C.J. (2015), "A study on the effect of tunnelling to adjacent single piles and pile groups considering the transverse distance of pile tips from the tunnel", *J. Korean Tunn. Undergr. Sp. Assoc.*, **17**(6), 637-652. https://doi.org/10.9711/KTAJ.2015.17.6.00.

Jeon, Y.J., Kim, S.H., Kim, J.S. and Lee, C.J. (2017), "A study on the effects of ground reinforcement on the behaviour of pre-existing piles affected by adjacent tunnelling", *J. Korean Tunn. Undergr. Sp. Assoc.*, **19**(3), 389-407. https://doi.org/10.9711/KTAJ.2017.19.3.389.

Jeon, Y.J., Kim, J.S., Jeon, S.C., Jeon, S.J., Park, B.S. and Lee, C.J. (2018), "A study on the behaviour of single piles to adjacent Shield TBM tunnelling by considering face pressures", *J. Korean Tunn. Undergr. Sp. Assoc.*, **20**(6), 1003-1022. https://doi.org/10.9711/KTAJ.2018.20.6.1003.

Jeon, Y.J., Jeon, S.C., Jeon, S.J. and Lee, C.J. (2020a), "Study on the behaviour of pre-existing single piles to adjacent shield tunnelling by considering the changes in the tunnel face pressures and the locations of the pile tips", *Geomech. Eng.*, **21**(2), 187-200. https://doi.org/10.12989/gae.2020.21.2.187.

Jeon, Y.J., Jeon, S.C., Jeon, S.J. and Lee, C.J. (2020b), "A study on the behaviour of pre-existing single piles to adjacent shield TBM tunnelling from three-dimensional finite element analyses", *J. Korean Tunn. Undergr. Sp. Assoc.*, **22**(1), 23-46. https://doi.org/10.9711/KTAJ.2020.22.1.023.

Jeon, Y.J., Lee, G.S., Lee, J.C., Batbuyan, C. and Lee, C.J. (2022), "A study on platform-based preliminary design guidelines associated with the behaviour of piles to adjacent tunnelling", *J. Korean Tunn. Undergr. Sp. Assoc.*, **24**(2), 129-151. https://doi.org/10.9711/KTAJ.2022.24.2.129.

Jeon, Y.J. and Lee, C.J. (2023). "Analysis of pile group behaviour to adjacent tunnelling considering ground reinforcement conditions with assessment of stability of superstructures", *Geomech. Eng.*, **33**(5), 463-475. https://doi.org/10.12989/gae.2023.33.5.463.

Kaalberg, F.J., Teunissen, E.A.H., Van Tol, A.F. and Bosch, J.W. (2005), "Dutch research on the impact of shield tunneling on pile foundations", *Proceedings of the 16th International Conference on Soil Mechanics and Geotechnical Engineering*.

Lee, C.J. and Chiang, K.H. (2007), "Responses of single piles to tunnelling-induced soil movements in sandy ground", *Can. Geotech. J.*, **44**(10), 1224-1241. https://doi.org/10.1139/T07-050.

Lee, C.J. (2012a), "Three-dimensional numerical analyses of the response of a single pile and pile groups to tunnelling in weak weathered rock", *Tunn. Undergr. Sp. Tech.*, **32**, 132-142. https://doi.org/10.1016/j.tust.2012.06.005.

Lee, C.J. (2012b), "Behaviour of single piles and pile groups in service to adjacent tunnelling conducted in the lateral direction of the piles", *J. Korean Tunn. Undergr. Sp. Assoc.*, **14**(4), 337-356.

Lee, C.J. (2012c), "The response of a single pile and pile groups to tunnelling performed in weathered rock", *J. Korean Soc. Civil Engineers*, **32**(5), 199-210. https://doi.org/10.12652/Ksce.2012.32.5C.199.

Lee, C.J. (2013), "Numerical analysis of pile response to open face tunnelling in stiff clay", *Comput. Geotech.*, **51**, 116-127. https://doi.org/10.1016/j.compgeo.2013.02.007.

Lee, C.J., Jeon, Y.J., Kim, S.H. and Park, I.J., (2016), "The influence of tunnelling on the behaviour of pre-existing piled foundations in weathered soil", *Geomech. Eng.*, **11**(4), 553-570. https://doi.org/10.12989/gae.2016.11.4.553.

Liu, C., Zhang, Z. and Regueiro, R.A. (2014), "Pile and pile group response to tunnelling using a large diameter slurry shield - Case study in Shanghai", *Comput. Geotech.*, **59**, 21-43. https://doi.org/10.1016/j.compgeo.2014.03.006.

Macklin, S.R. (1999), "The prediction of volume loss due to tunnelling in overconsolidated clay based on heading geometry and stability number", *Ground Eng.*, **32**(4), 30-33.

Mair, R.J. and Williamson, M.G. (2014), "The influence of tunnelling and deep excavation on piled foundations", *Geotechnical Aspects of Underground Construction in Soft Ground*, Seoul, Korea, August.

Marshall, A.M. (2009), "Tunnelling in sand and its effect on pipelines and piles", Ph.D. Thesis, University of Cambridge, Cambridge, U.K.

Mroueh, H. and Shahrour, I. (2008), "A simplified 3D model for tunnel construction using tunnel boring machines", *Tunn. Undergr. Sp. Tech.*, **23**(1), 38-45. https://doi.org/10.1016/j.tust.2006.11.008.

Ng, C.W.W., Lu, H. and Peng, S.Y. (2013), "Three-dimensional centrifuge modelling of the effects of twin tunnelling on an existing pile", *Tunn. Undergr. Sp. Tech.*, **35**, 189-199. https://doi.org/10.1016/j.tust.2012.07.008.

Ng, C.W.W. and Lu, H. (2014), "Effects of the construction sequence of twin tunnels at different depths on an existing pile", *Can. Geotech. J.*, **51**(2), 173-183. https://doi.org/10.1139/cgj-2012-0452

Ng, C.W.W., Soomro, M.A. and Hong, Y. (2014), "Three-dimensional centrifuge modelling of pile group responses to side-by-side twin tunnelling", *Tunn. Undergr. Sp. Tech.*, **43**, 350-361. https://doi.org/10.1016/j.tust.2014.05.002.

Pang, C.H. (2006), "The effects of tunnel construction on nearby pile foundation", Ph.D. Thesis, The National University of Singapore, Singapore.

Phienwej, N., Sirivachiraporn, A., Timpong, S., Tavaranum, S. and Suwansawat, S. (2006), "Characteristics of ground movements from shield tunnelling of the first Bangkok subway line", *In Proceedings of the International Symposium on Underground Excavation and Tunnelling*, Bangkok, Thailand, February.

Plaxis 3D (2024), *Reference Manual, in Plaxis 3D User's Manual.*

Selemetas, D. (2005), "The response of full-scale piles and piled structures to tunnelling", Ph.D. Thesis, University of Cambridge, U.K.

Selemetas, D. and Standing, J.R. (2017). "Response of full-scale piles to EPBM tunnelling in London Clay", *Géotechnique*, **67**(9), 823-836. https://doi.org/10.1680/jgeot.SIP17.P.126.

Soomro, M.A., Ng, C.W.W., Memon, N.A. and Bhanbhro, R. (2018), "Lateral behaviour of a pile group due to side-by-side twin tunnelling in dry sand: 3D centrifuge tests and numerical modelling", *Comput. Geotech.*, **101**, 48-64. https://doi.org/10.1016/j.compgeo.2018.04.010.

University of Cambridge : 2020 Case studies. (2020), https://www-smartinfrastructure.eng.cam.ac.uk/projects-and-case-studies/2020-case-studies/monitoring-under-reamed-piles-during-tunnelling.

Wang, X. and Yuan, D. (2022). "Research on the interaction between the pile and shield machine in the process of cutting a reinforced concrete pile foundation", *Appl. Sci.*, **13**(1), 245. https://doi.org/10.3390/app13010245.

Williamson, M.G. (2014), "Tunnelling effects on bored piles in clay", Ph.D. Thesis, University of Cambridge, Cambridge, U.K.

Zhang, C., Zhao, Y., Zhang, Z. and Zhu, B. (2021), "Case study of underground shield tunnels in interchange piles foundation underpinning construction", *Appl. Sci.*, **11**(4), 1611. https://doi.org/10.3390/app11041611.